SLAC-PUB-6717
November 1994
(A/I)

The Wire Scanner System of the Final Focus Test Beam*

Clive Field

Stanford Linear Accelerator Center, Stanford University, Stanford, CA 94309, USA

Abstract

The system of wire scanners in use at the FFTB at SLAC is described. In addition to the scanners themselves, there is a discussion of detectors for the scattering from the wires, and of the procedure for handling beam spots of large aspect ratio.

Submitted to *Nuclear Instruments and Methods in Physics Research*

*Work Supported by US Department of Energy, contract DE-AC03-76SF00515.

1. Introduction

Wire scanners have become increasingly important in the tool chest of diagnostic equipment for high energy particle beams. Various types have been developed for use with the pulsed beam at the SLC.[1-5] This note contains a summary of the suite of scanners for the Final Focus Test Beam at SLAC, and examines some new aspects of the subject.

The Final Focus Test Beam is an external electron beam line from the SLAC linac.[6] It is designed to make use of the low emittance delivered by the damping rings and hardly diluted in the linac. The linac beam, at 46.6 GeV, is directed at near zero degrees into a five-stage beam line where a demagnification of more than 300 leads to spot sizes as small as 60 nm in the vertical plane. The beam line and its systems are a test of the techniques needed to deliver beams to the interaction point of a possible future collider while maintaining the specifications for high luminosity.

Figure 1 shows schematically the positions of the wire scanners and related equipment along the beamline. The first stage of the line is intended to match the beta of the incoming beam to the lattice of the test beam. Near the end of this section a beam focus can be arranged. It is measured by the first wire scanner station.

Since the final focussing doublet in the test beam is so strong, the momentum dependence of its focus has to be cancelled accurately in horizontal and vertical planes. For the horizontal axis, this occurs in the second stage of the line (CCSX — Chromatic Correction Section X-axis). It is done by dispersing the beam, and using a pair of sextupoles which are separated by half of a betatron wavelength to cancel geometric aberrations.

The third section rematches the betatron function, from $\beta_x \gg \beta_y$ to the inverse, for the following vertical chromatic correction section. There are separated horizontal and vertical foci in section three, and a wire scanner is placed at each for diagnostics on the horizontal chromatic correction. The spot sizes at these foci, and particularly their aspect ratios (Table 1), have required special attention in the design of the scanners.

The fourth part of the beam line (CCSY) cancels the chromatic error in the vertical plane. Although a focus can be made accessible after this section, the nominal size and aspect ratio of the beam, $\sigma_y \times \sigma_x \doteq 0.5\ \mu\text{m} \times 2000\ \mu\text{m}$, is beyond the range that can economically be handled at present.

The size is also too small after the final stage (FT — Final Transformer), where the strong quadrupoles have a focal length of only ~1.5 metres and the spot size, fully optimized, is $\sigma_y \times \sigma_x = 0.06\ \mu\text{m} \times 1\ \mu\text{m}$. The beam can be focussed on either of two other devices that have been developed for these conditions [7,8], but a scanner station has also been provided for assistance during initial set up, and for diagnostics. In addition, a scanner has been placed 540 mm downstream of the focal point, before any magnetic elements intervene, to measure the beam divergence.

There is actually one further stage in the beam — it must be transported to a dump. This is accomplished by another section of optics, arranged as a relay lens followed by a downward bend so that muons from the dump are directed into the ground. At the relay focus just in front of the dump, where the momentum dispersion is 605 mm, is placed one more wire scanner whose purpose is to measure the momentum spectrum of the beam.

A summary of the FFTB scanners and their design requirements is given in Table 1.

Table 1.
Wire scanner positions, functions and spot sizes.

Scanner station	Location	Purpose	Nominal beam size when tuning with scanner $\sigma_x \times \sigma_y$
W.S. 1	Near end of β-match	β, emittance	15μ×10μ (minima)
W.S. 2	X-focus in β-exchange	α_x, β_x, η, CCX sextupole alignment	3μ (minimum) ×90μ
W.S. 3	Y-focus in β-exchange	α_y, β_y	360μ×0.9μ (minimum)
Focal point scanner	main focus	Initial tuning	≥ 1.5μ×1.5μ (minima)
Divergence scanner	54 cm downstream of main focus	Divergence measurement	~190μ×300μ
Energy spectrum scanner	Focus near dump	Energy spectrum	0.02mm×2mm

2. General Considerations

The FFTB beam pulse, a few picoseconds long, has a repetition rate limited to 30 Hz. For this reason it is appropriate to move the wires in steps between beam pulses. For most of the scanners this is accomplished by using a stepping-motor-driven linear motion stage and a CAMAC stepping motor controller.[9] The current pulses are driven conventionally from a separate power supply and limiting resistors. All the electronics are outside the radiation area, with long cables stretching to the scanners. The system was designed to be compliant with the SLC control program, using standard electronics and software. In one case — the focal point scanner station — the stepping motor system is not used because of space constraints. Instead, small electromagnets are used to step the beam trajectory across the wire, as is done at the SLC interaction point.[2,3]

A drawing, Fig. 2, illustrates wire scanner 2 (WS2), and is representative of the stepping mechanisms. A principle of the design is that inertia is kept as low as is consistent with rigidity. The linear motion stage[10] is rigidly fixed to the beam pipe using a plate and clamps. The stage carries a metal block to which in turn is welded the vacuum bellows and the rod which penetrates into the vacuum. A constant-force spring motor is used partially to counteract the pressure on the vacuum bellows (except for vertical scan axes where the weight of the moving parts does the job).

At the end of the rod is clamped the fork which holds the fine wires. The vacuum rod axis is kept as close as practical to the screw axis of the stage in order to minimise vibration or flexure with a component parallel to the direction of motion, that is, to the beam measurement direction. Vibration in this direction is limited to settling of the motor into its magnetic detent position, transmitted through the gear train. The operational procedure of stopping the motor at each beam pulse is intended to suppress resonance in this vibration, a well known risk in stepping motor systems at low speed. A full acceleration-coast-deceleration cycle is used. No evidence of vibration difficulties has been seen in normal operation.

The selection of the material, number, size and layout of the fine wires was made individually for each scanning station, and the forks were designed to suit. They have a common design basis, however. The individual forks were machined out of 3.2 mm thick Macor[11], whose surface was, in the end, coated with graphite. With a resistance in the range of 1 MΩ per square, this is a way to bleed off radiation-induced surface charge. As illustrated in Fig. 3, the wires were positioned on terraces machined as circular arcs, a fraction of a millimeter deep, into the Macor. These set a conservative bending radius of the wires, while positioning them to 10 microns or better. The machining was done inexpensively on a numerically controlled mill.

Vacuum and radiation considerations precluded the use of organic materials for attaching the wires. Instead, Sn96 tin-silver solder was used without flux. Gold plated copper tabs, 0.125 mm thick, were screwed on to the Macor and bent over the side. The wires were strung over the terraces and down across the tabs, where they hung under the tension of small weights. They were then encapsulated in solder at the tabs. Note that this technique works for both carbon fibres and unplated tungsten wires. This procedure also took care of the mandatory grounding of the wire. In some cases it was desirable to prevent wires from slipping off the terraces by applying a minute quantity of a vacuum qualified ceramic cement.

The most robust and bias-free signal of the overlap between the beam and a wire, Bremsstrahlung, is at zero opening angle relative to the electron beam. Fortunately there are dipoles downstream of all but the last of the scanners, and the beam electrons are deflected enough to allow access to the Bremsstrahlung gamma rays. Since, however, the gamma ray counters are in a swath of synchrotron radiation, additional counters of the same design have been positioned to measure the flux of Bremsstrahlung electrons deflected out of the beam pipe by the dipoles. Descriptions of the detectors are included below with discussions of the individual scanning stations.

3. Characteristics of Individual Scanners

3.1 Wire Scanner Station 1

The minimum beam dimensions are listed in Table 1, and show that, for the first scanner station, step sizes of a few microns are needed. The design beam spots are not far from round, and so, to reconstruct the two-dimensional beam size ellipse, including its roll angle, it is best to scan in the horizontal (x), vertical (y) and 45° (v) axes. A station was built using three independent scanners of the type described above. In fact it was possible to reuse some components described in Ref. 1.

The linear motion stages[10] have a step size of 1 μm. All three sets of fibres can be on, or close to, the beam at the same time, with a displacement along the beam line of 6 mm between x- and y-forks and 38 mm to the v-fork.

The evidence at SLC is that carbon fibres are broken by beams of approximately 10^{10} electrons with $\sigma_x \times \sigma_y < 3\ \mu m^2$. Calculations for tungsten suggest that it should withstand perhaps an order of magnitude less superficial beam intensity. Although this would appear to qualify tungsten for the first station, the conservative choice was to use carbon despite its lower Bremsstrahlung yield. On each fork, a thick fibre, 34 μm diameter, was provided for beam-finding and the measurement of wide beam spots. Since the rms width of a circle is (diameter/4), a wire of diameter 7 μm would widen the measured rms width of a 5 μm beam by only 6%. Since 7 μm carbon fibres are easily available, these have been chosen for measuring the smaller spots at the first wire scanner. In fact four of these thin fibres, in addition to the 34 μm fibre, are spaced at 380 μm on the forks for this set of scanners. It is worth mentioning that, before operation, there were concerns about Bremsstrahlung signal levels from the thin carbon, relative to possible background. As a backup, one end of each of the thin fibres has been connected through the vacuum wall, thus retaining the ability to read the charge depletion signals from them. The fibre's other end has been connected to ground on the fork, using a surface mount chip resistor of about 0.15 MΩ.

The Bremsstrahlung gamma rays from this scanner pass through the dipoles downstream, and exit the vacuum pipe in a $\pm 3\sigma$ beam of 4 mm × 0.7 mm. The exit is through a perpendicular, 10 mm thick, stainless steel "window" which prevents problems with grazing incidence on the beam pipe. As noted above, the gamma rays compete with synchrotron radiation from the dipoles — in fact this first gamma ray counter is looking effectively straight up the full length of the linac. The electron counter in this case is separated by 60 mm from the gamma counter, centre to centre. The off-energy electrons (30-20 GeV) also have a small perpendicular window to simplify the understanding of their exit from the beam pipe.

The counter design is illustrated in Fig. 4. A shower converter, lead in this case, 12.5 mm thick at 45°, precedes a length of 25 mm air. This is used as a Čerenkov emission medium, and it terminates in a 45° mirror made of polished aluminum. The cross-section of the initial light channel is 25 mm × 25 mm and this is increased after each additional 90° reflection to retain rays within 7° of the axis. There is a total of three 45° mirrors before the light reaches a cavity containing a photomultiplier tube. The light path is 1 m long. The walls of the Čerenkov section and the first few centimetres of the light pipe are painted flat black. Beyond that, the walls have been made highly reflective by applying aluminized Mylar. The p.m.t.s[12] were chosen for their ability to drive large peak currents, and the voltage division was selected to optimise this for gains in the range 10^4. The tubes operate at 1500 to 1800 V. Starting before the second mirror, and especially around the front face of the p.m.t., the light path of each counter is heavily shielded by lead.

A pneumatically actuated plate, controlled remotely, can be driven across the light path. The plate has a regular pattern of 35 holes which attenuate the light signal by a factor of ten. This, of course, is available to prevent p.m.t. space charge saturation which can occur with small beam spots and tungsten wires.

The signals are taken directly out of the FFTB tunnel over RG214 cable to a CAMAC crate of the SLC data collection system. The dynamic range of the 11-bit ADCs is extended by passively splitting the signal in the ratio 10:1, and digitising each version in an ADC channel.

It has been found that, for the first wire scanner station, the gamma ray counter is subject to a variable and unpredictable background, occasionally sufficient to hide the signal of a wire scan. Fortunately the electron detector, separated from it by 2 cm of beam pipe, is relatively unaffected. An example of the profile of a scan is shown in Fig. 5.

3.2 Wire Scanners 2 and 3

The characteristically large aspect ratios at the next two scanners require a different treatment. The approach taken is to scan the beam with three wires mounted with slightly different angles to the principal axis of the nominal beam spot ellipse.

The formalism assumes that the beam ellipse is eccentric enough that the small angle approximation is good, and that the second and third wires have an equal and opposite (small) angle relative to the first.

θw is the absolute value of the angle of the second and third wires relative to the first.
θt is the tip angle of the beam ellipse relative to wire #1.
σL and σN are the long and narrow gaussian widths of the beam. σN will be nearly perpendicular to the first wire.
$\sigma 1,2,3$ are the widths of the three peaks from the sequential scans of wires 1,2 and 3. Wire 1 is the 0° wire.
σw is the RMS effective radius of the wires. The uncertainty in σw is assumed to be negligible.

Some factors are used repeatedly, so define:

$$D = \sigma 3^2 + \sigma 2^2 - 2\sigma 1^2$$

$$S32 = (\sigma 3^2 - \sigma 2^2)$$

It is easier to work in terms of the SQUARES of the beam widths. The solutions are:

$$\sigma L^2 = D \ / \ (2 \times \theta w^2)$$

$$\sigma N^2 = \sigma 1^2 - S32^2 \ / \ (8 \times D) - \sigma w^2$$

$$\theta t = \theta w \times S32 \,/\, (2 \times D)$$

Although in the interests of brevity the formal expressions will not be given here, the uncertainties are propagated from the uncertainties of the gaussian widths in the three fits to the scanned peaks, $\delta\sigma 1$, $\delta\sigma 2$, $\delta\sigma 3$. As in the case of the beam widths, it is easier to derive expressions for the partial derivatives of their squares. In the case of σL^2, there is a substantial simplification since $\sigma w \ll \sigma L$.

A simulation study was carried out with a wide range of x- and y- sizes and angles of the beam ellipse. The results were used to select angles for the wires. The criterion was the maintenance of acceptable uncertainties in the solution of the beam spot ellipse, over the range of actual beam shapes and sizes likely to be encountered. For the vertical focus after the first chromatic correction section (WS2), a triplet of wires has been provided at -3°, 0° and +3° relative to the vertical axis. A second triplet, for occasions when the aspect ratio is considerably smaller than nominal — and to act as a spare — is also installed, with angles double those of the first. In the case of the horizontal focus, WS3, the selected angles were 0.7° for the first triplet, and 1.4° for the second.

At these scanners, the superficial intensity of the beam does not raise concerns about damage to tungsten wires. Those used were without surface cladding, and of diameter 4 μm, as small as could easily be found and handled. In fact, one wire broke during beam studies, not where the beam could touch it, but at the tangent to the Macor at the end of its span. The failure mechanism is not understood.

The scanner for the horizontal beam profile can satisfactorily use a minimum step size of 1 μm, as described above. But for WS3, scanning vertical profiles of rms width 1 μm or less, a finer step size is needed. This has been arranged by using a different gear train between the standard stage type and motor. The steps are 0.1 μm. The stage's linear speed is similarly reduced, however. It is quick enough during scans of the beam, but takes too long to cover the 2.5 cm between the safe retracted position and the starting point of scans, close to the beam. This difficulty is obviated by simply mounting a small, pneumatically actuated, stage on the stepping stage, and mounting the scanner hardware on the pneumatic device. The latter forces the scanner fork 2.5 cm towards the beam when needed, and the whole thing is stepped by the lower stage to scan the wires across the beam.

Some effort has been expended to examine the stepping motion of WS3. Three techniques have been used. Two of these were work-bench tests. A knife-edge fixed to the stage was made to cut a laser spot, and the light passing to a photodiode was recorded as the stage was started, run for a few pulses, and stopped. If the motion was maintained long enough, a longitudinal resonance was observed at close to 100 Hz. A different device[13] was used to test the uniformity of the pulse-by-pulse motion over wide ranges. This indicated an occasional loss of 100 nm, the least count. It perhaps relates to elasticity in the measuring tooling, but, alternatively, to steps missed during the repeated acceleration from rest. It was randomly distributed along a scan. Although demonstrating reliability at the 100 nm level would require more work, it is not an issue for scanning at the 1 μm level. A final examination was made *in situ* by sampling the position indication of the LVDT as frequently as possible during representative scans. Again, with a sensitivity sufficient for scans of 1 μm beams, no anomalies were found.

There are no magnets between the scanners at these two foci, and so they share Bremsstrahlung detectors of the design described above. The tungsten wires, together with beam spots that are small in the direction of the scan, give rise to Bremsstrahlung fluxes a hundred times higher than from the 7 μm fibres of the first set of scanners. For this reason the gamma ray counter for scanners 2 and 3 has brass rather than lead for its shower converter, and its pinhole attenuator transmits only 1.4% of the light. When properly aligned and operated so as not to saturate with the large signal, the electron and gamma ray counters report identical measurements of the beam shape.

Fig. 6 is an example of a measurement of the vertical spot size using WS3. In Table 2 is illustrated the reconstruction of the beam ellipse from a triplet of scans.

Table 2.
Results from 3-wire measurement of a large aspect ratio beam at the third wire scanner. The beam profile is narrow vertically, wide horizontally. Dimensions are in microns unless otherwise indicated.

Measurement	σ1	δσ1	σ2	δσ2	σ3	δσ3
	0.884	±0.03	2.82	±0.03	2.27	±0.03
Solution	σN	δσN	σL	δσL	θ	δθ
	0.834	±0.068	199	±3	0.084°	±0.007°

3.3 Focal Point Scanners

Two sets of scanners are used to study the beam at the focal point. The beam can be focussed at the position of one of the sets, which can be used to study the spot size down to about 800 nm × 2 μm. The second scanner, 537 mm downstream, measures the spot size after it has diverged, and gives the divergence angles which are typically $\sigma_y \times \sigma_x = 550 \times 350$ μrad..

The first of these stations uses a simple and compact pneumatic system to position a set of fibres on to the beam line. Either horizontal or vertical fibres can be chosen for scanning, and, as stated above, the beam is deflected magnetically across the stationary fibres. For each axis there are 10 fibres, spaced 50 μm apart, on a Macor fork of the usual type. In this way space and access requirements for other equipment in the focal point area could be met.

Because the small electron beam is destructive, carbon was the material of choice, but the diameter of the fibres varies by more than ±10%. The diameters of those on the forks were measured, where the electron beam would hit them, using fringes in the diffracted beam from a focussed laser spot. This technique was also used to check the considerably more uniform diameter of the thin tungsten wire. Care had to be taken with beam polarisation, since reflection from the target surface, with its phase shift, causes a polarisation-dependent shift in the fringes, requiring a correction.[14]

The destructive effect of the beam is illustrated in Fig. 7. This electron micrograph shows the end of a fibre which was cut by beam pulses of about 6×10^9 electrons in a spot size of

$\sigma_y \times \sigma_x \sim 600$ nm $\times$ 2 μm. The wide axis of the beam was parallel to the fibre. As shown in Fig. 8, the beam was steered in 0.5 μm steps across the wire to the point of destruction. In the other case, Fig. 9, the wide axis was perpendicular to the fibre, and of roughly comparable width. The clean, sliced cut in this case contrasts strongly with the mangled carbon of Fig. 7.

For the divergence measurement, where beam sizes in the range of 30 - 300 μm are encountered, available space limited the design to a single scanning axis. Thus the scan is performed at 45° between the y- and x- axes, and the fork carries three fibres, one parallel to either axis and one perpendicular to the scan direction. Since the eccentricity at this scanner is not very large, the spot ellipse can readily be reconstructed. The scan range is relatively large, and so the motor and gearbox were selected for 10 μm steps, and consequently enhanced speed.

Both the focal point scanner and this divergence scanner must share downstream Bremsstrahlung detectors, and so, rather than tungsten, carbon fibres of diameter 34 μm were selected for the divergence measurement. This reduced the dynamic range needed from the detectors.

Downstream of the focal point, the electron beam is first collected by a train of quadrupoles, and then deflected downward by 17.4 mrad. At 33.0 metres from the focal point, there is space for a detector which can cover the full vertical divergence cone to $\pm 3\sigma$. At the analogous places at SLC[15] there are serious difficulties with synchrotron radiation and gamma ray backgrounds, extending off beam-axis, caused by beam tails scraping apertures far upstream. Although the synchrotron radiation from the FFTB dipoles has a critical energy of 0.5 MeV, 1/3 that at SLC, and its total energy is lower by a similar fraction, there is a contribution from the powerful quadrupoles which extends to higher energies and varies with the beam tuning. Concerns about the other backgrounds remain. These are particularly a risk for large aperture counters.

The detector is illustrated in Fig. 10. Since the gamma rays exit the vacuum pipe through an aluminum plate of only 2% of a radiation length, a converter of 2 radiation lengths of lead is provided. Air is again used as the Čerenkov medium, this time with a length of 260 mm. The optics, installed in the blackened cavity of the counter body, is designed to image the electron beam focal point on to the face of a p.m.t.. The angular spread of shower tracks above the 25 MeV threshold is accommodated by the acceptance. Since divergence measurements are an important part of its task, geometric uniformity of response is emphasized. The primary mirror was fabricated from a plate of aluminum by single point diamond turning. Its focal length is 650 mm, and its dimensions are 108 $\times$ 159 mm. There are two secondary plane mirrors, of aluminised black acrylic, which fold the light path through a circular aperture intended to exclude unwanted scintillation light, and on to the p.m.t. face. A 2-inch diameter Philips XP2020 p.m.t. is used, with a base chosen, again, for linearity with large pulses. About 85 kg of lead are included in the counter body to shield the tube, and the device is also shielded externally.

An electron counter, of the same design as for the upstream scanners, is also positioned to accept electrons escaping the beam pipe with energies about 33 to 36 GeV.

The plot of Fig. 11 exemplifies the measurement of a small spot at a 4.3 μm carbon fibre at the focal point, using the gamma ray detector.

3.4 Energy Spectrum Scanner

The final scanner, just in front of the beam dump enclosure, is somewhat different from the others. The vertical size of the dispersed beam spot can be up to 5 mm, if a wide energy spectrum is being transmitted. Since Bremsstrahlung is not accessible, the primary mechanism for measuring the beam size was chosen to be the production and multiple scattering of delta rays in the material scanned across the beam. The scattering step is obviously enhanced by using material with short radiation length. In this device a ribbon of tungsten was used, 75 μm thick perpendicular to the beam, and 2 mm wide along the beam direction. This arrangement readily allowed scattered delta rays to escape the tungsten. Some of those at about 1 MeV were able to escape the vacuum pipe through a 50 μm stainless steel window, and pass through the aperture of a lead collimator to a heavily shielded photomultiplier.[16] Čerenkov light in the front face provided the signal. An example of a beam profile is shown in Fig. 12.

In addition to the ribbon, a grid of 24 wires, each 175 μm diameter of beryllium-copper, spaced at 305 μm transverse to the beam, was mounted on the same positioning rod. Because of the extra mass, longer stroke and higher speed required, a more powerful stage was used than for the other scanners.[17] The wires were mounted on six Macor forks of the standard type, four to a fork. They were spaced longitudinally to minimise interference between wires, either cross talk of their secondary emission, or local space charge effects. The wires on each fork were ganged electrically and their secondary emission signals brought through the vacuum wall to preamplifier/shapers described in Ref. 1. The 3 μs time constant averages out the bipolar signal of the substantial radiofrequency noise, while retaining the charge depletion secondary electron signal. This can be used as a backup for scanning. However, if the grid is left in position across the beam, it provides a continuous monitor of the spectrum width, and also, at low resolution, of gross shape changes. An example of the shape from a single beam pulse, using the six channels, is shown in Fig. 13.

4. Acknowledgements

The successful operation of this equipment owes much to the excellent technical work of Karl Bouldin and Yung-Yung Sung. The thoughtful design drawings of Jim Lewis and Melvin Marter were invaluable. We are indebted to Nancy Spencer, Linda Hendrickson and Greg Sherwin of the SLC programming staff for their work in integrating this system into the SLC control program and database. The SLC operators and the FFTB collaboration have already brought the beam line close to its design performance, and in doing so have made the scanner suite into a useful tool.

References

[1] R. Fulton et al., Nucl. Instr. and Meth., A274 (1989) 37;

[2] G. Bowden at al., Nucl Instr. and Meth., A278 (1989) 664;

[3] C. Field et al., Nucl. Instr. and Meth. A295 (1990) 279.

[4] D. McCormick et al., SLAC-PUB-6615, October 1994, SLAC, Stanford, CA94309, U.S.A.

[5] M.C. Ross et al., "Experience with Wire Scannners at SLC", Proceedings of Accelerator Instrumentation Workshop, Berkeley, 1992, AIP Conf. Proc. 281 (1993) p. 264.
[6] Final Focus Test Beam Design Report, SLAC-376, March 1991, SLAC, Stanford, CA 94309, U.S.A.
[7] J. Buon et al., Nucl. Instr. and Methods A306 (1991) 93.
[8] T. Shintake, Nucl. Instr. and Methods A311 (1992) 453.
[9] Joerger Enterprises Inc., East Northport, NY 11731, U.S.A., model SMC-24BPSMC
[10] Klinger Scientific, Garden City, NY 11539, U.S.A., stage UT100.75 PP.
[11] Corning Glass Works, Corning, NY 14830, U.S.A., Macor machinable glass ceramic.
[12] Philips Photonics, Statersville, RI 02876, U.S.A., p.m.t. XP2012B. Resistor values from photocathode to anode (kΩ): 308, 154, 25, 154, 187, 187, 226, 332, 332, 383, 332.
[13] Heidenhain Corporation, Elk Grove Village, Il 60007, U.S.A., model MT60 K with PC interface board IK120.
[14] Loren Hill, Dissertation for Degree of B.A. in Physics, Univ. of Cal., Santa Cruz, CA 95064, U.S.A.
[15] G. Bonvicini et al., Nucl. Instr. and Meth., A277 (1989) 297.
[16] Hamamatsu Corporation, Middlesex, NJ 08846, U.S.A., p.m.t. R1398.
[17] Klinger Scientific, stage MT160, range 100 mm, UE73 motor.

Figure Captions

1. The trajectory of the FFTB beam, shown in the horizontal and vertical planes (note the different scales of transverse and longitudinal axes). The positions of the wire scanners (listed as WS1, 2, 3, Focal Point, Divergence, and Energy Spectrum) are indicated, with the straight paths to the Bremsstrahlung detectors. The listed stages of the beam line are discussed in the text.

2. Perspective view of a representative wire scanner, shown with the beam vacuum pipe removed. For clarity, the LVDT and microswitches are not shown. To set the scale, the body of the stage is 205 mm long by 105 mm high.

3. Wire fork of Scanner 3. The terraced arcs on the Macor prongs are shown, accurately positioning six wires at various shallow angles. The gold-plated copper tabs and the solder capturing the wires are labelled. The width of the Macor is 25 mm.

4. Perspective view of a standard FFTB Bremsstrahlung detector with internal components drawn faint. The axis of the narrow gamma ray beam is seen at the top. It penetrates the shower converter, after which is a 25 mm long Čerenkov emission length. The mirrors are labelled 1,2 and 3. The pinhole light attenuator is shown, with its pneumatic actuator above it, and the p.m.t. is also indicated. The lower 1/3 of the device is encased in lead shielding. The height of the counter is 650 mm.

5. A vertical beam profile from a 7 μm carbon fibre of the first wire-scan station. The gaussian width is 7.9±0.3 μm.

6. A vertical beam profile from Wire Scanner 3. The gaussian width, after correcting for the 3.8 μm wire diameter, is 0.67±0.12 μm.

7. Secondary emission micrograph of a carbon fibre (approximately 4.3 μm diameter), severed by the electron beam. The major axis of the beam spot ellipse was parallel to the fibre. The footprints of the last 7 pulses across the fibre are indicated schematically by ellipse contours spaced by 0.5 σ.

8. Bremsstrahlung profile showing the sudden breakage of the fibre of Fig. 7. The smooth curve is the shape expected for a 0.6 μm r.m.s. beam and a 4.3 μm diameter fibre.

9. Secondary emission micrograph of a carbon fibre (approximately 4.3 μm diameter), severed by the electron beam with major elliptical axis perpendicular to the fibre axis. The footprints of the last 7 pulses across the fibre are indicated schematically with contours spaced by 0.5 σ.

10. Plan view of large acceptance Bremsstrahlung detector. The gamma ray beam axis is indicated. After the shower converter, light is emitted over 260 mm of air and is focussed by the concave mirror, by way of a periscope of two plane mirrors, on to the photomultiplier tube. The hatched area above the p.m.t. represents a lead shield.

11. A vertical beam profile measured with a carbon fibre at the FFTB focal point and the detector of Fig. 10. After correction for the wire diameter, the gaussian beam width is 0.66±0.18 μm.

12. Beam profile at the energy spectrum scanner. The full width at half maximum corresponds to 0.24 GeV.

13. Low resolution beam spectrum from the six bands of secondary emission wires. For this pulse, the fwhm corresponds to 0.22 GeV.

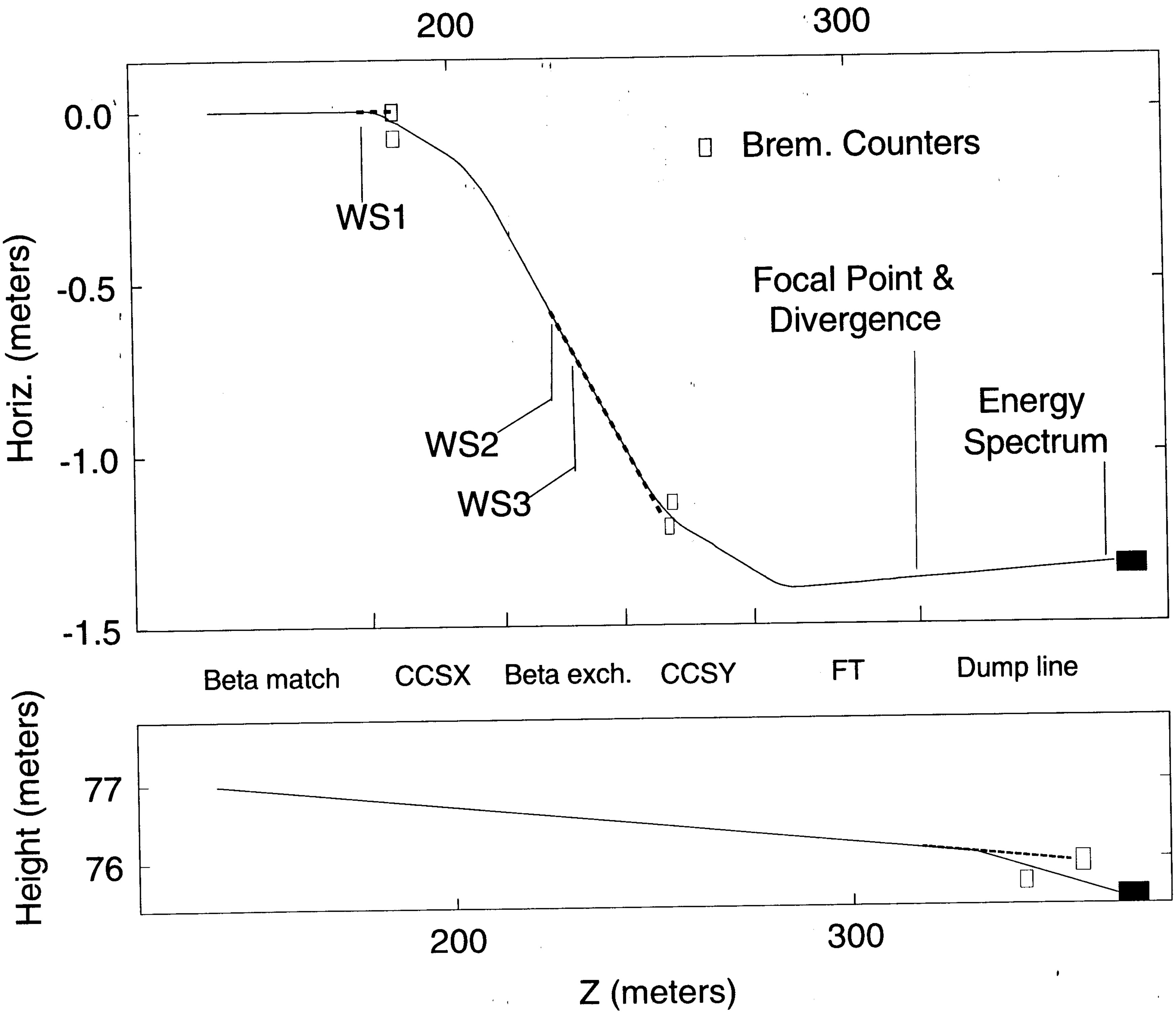
200
300
0.0
-0.5
-1.0
-1.5
Horiz. (meters)
Brem. Counters
WS1
WS2
WS3
Focal Point &
Divergence
Energy
Spectrum
Beta match
CCSX
Beta exch.
CCSY
FT
Dump line
Height (meters)
77
76
200
300
Z (meters)

Fig. 1

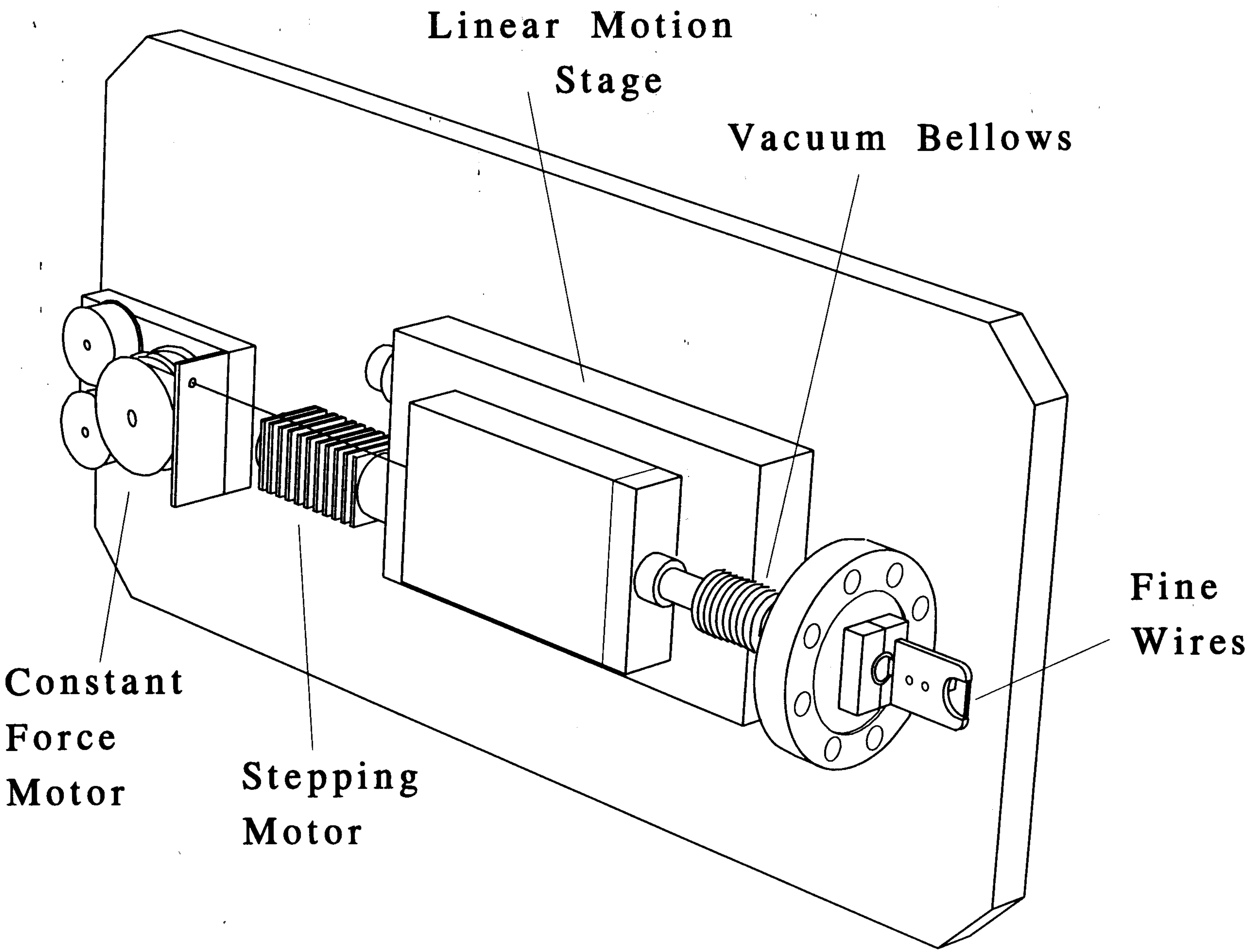
Linear Motion Stage
Vacuum Bellows
Fine Wires
Constant Force Motor
Stepping Motor

Fig. 2

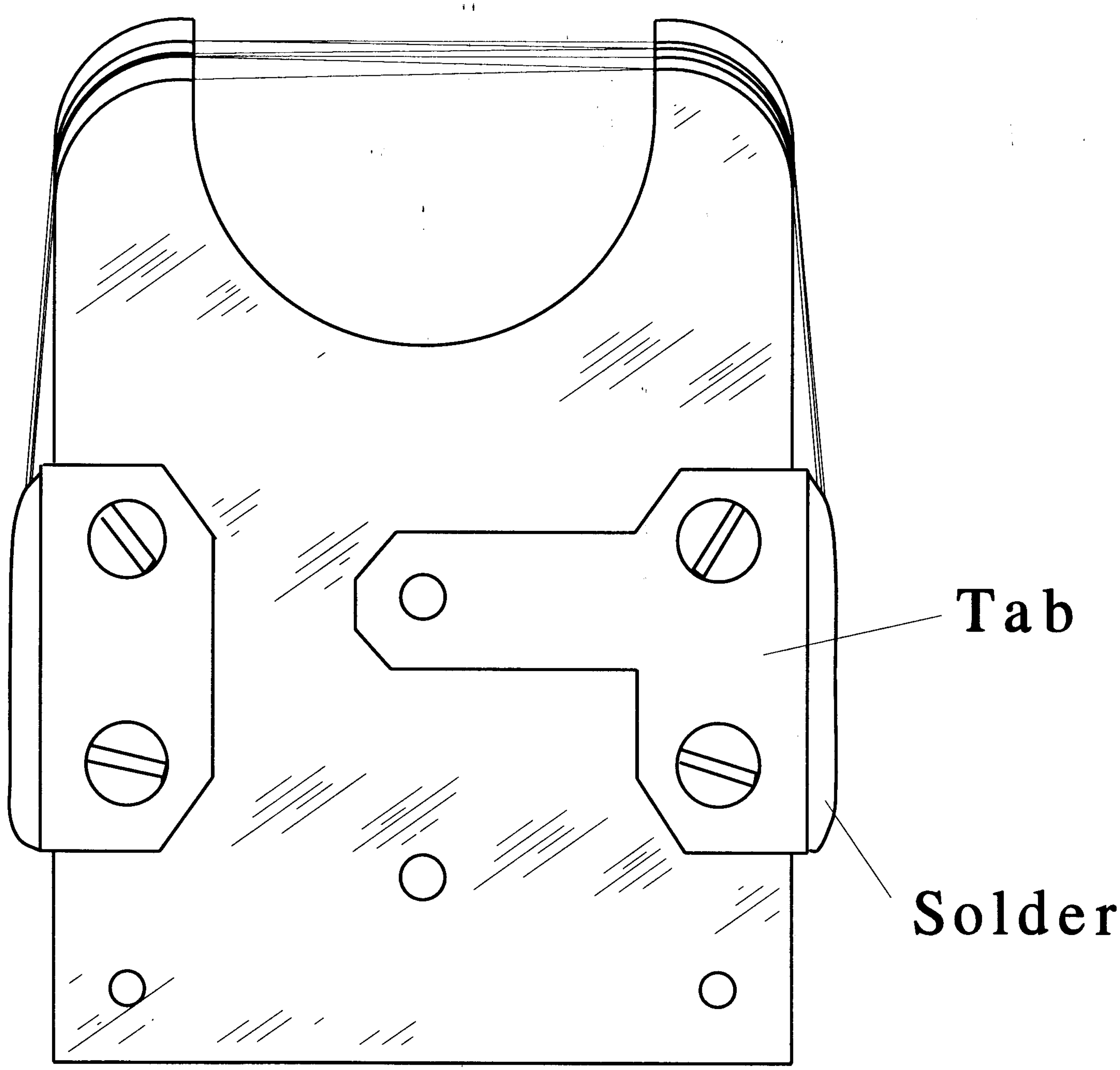

Fig. 3

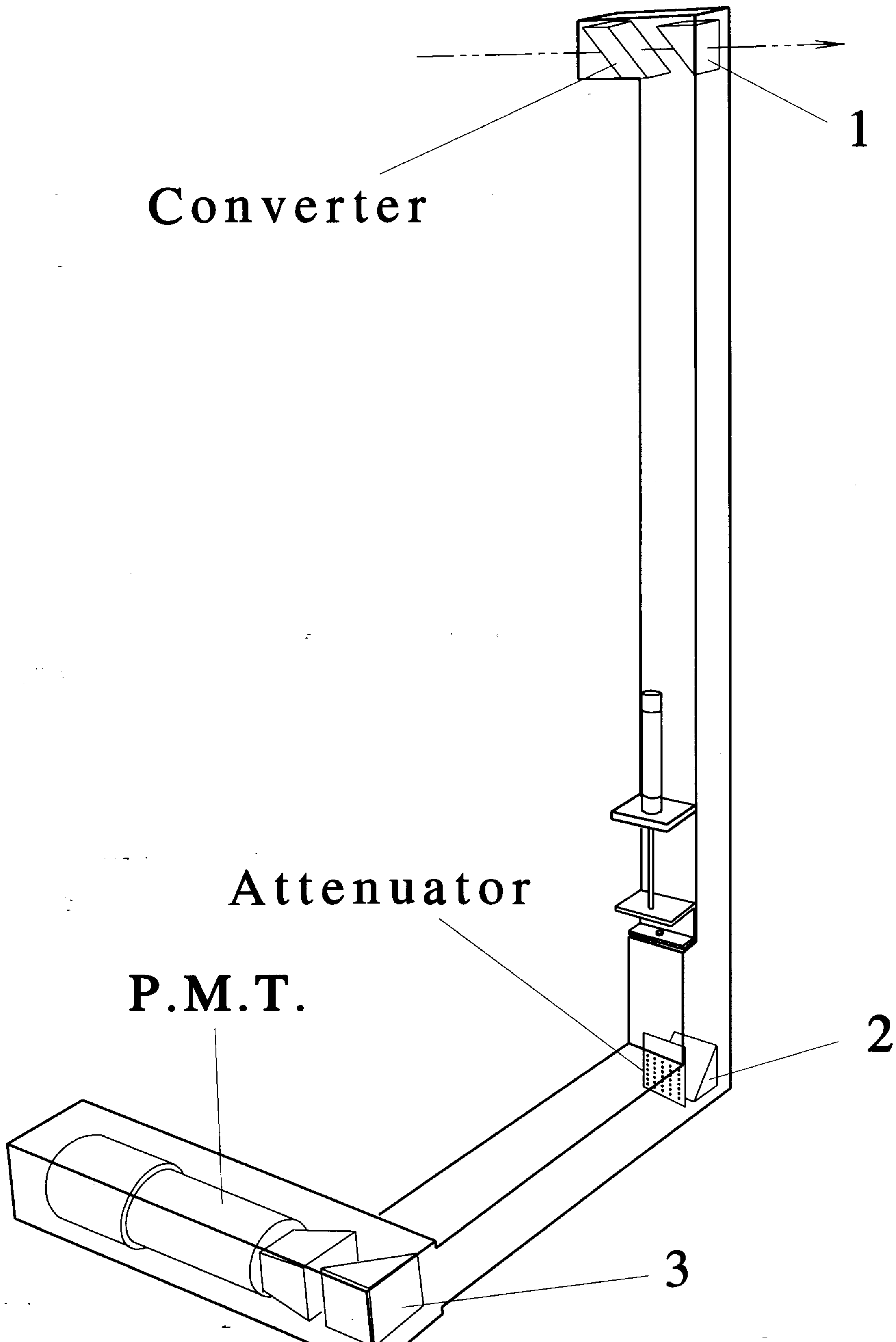

Fig. 4

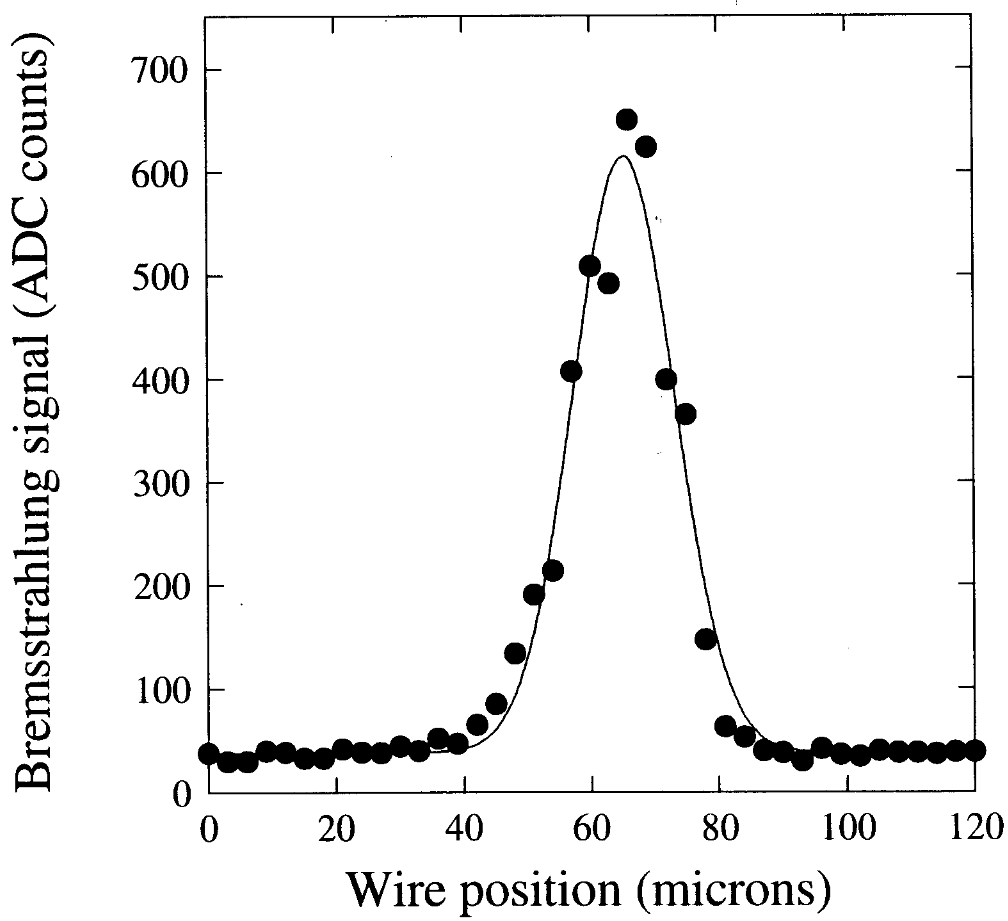

Bremsstrahlung signal (ADC counts)
700
600
500
400
300
200
100
0
0
20
40
60
80
100
120
Wire position (microns)

Fig. 5

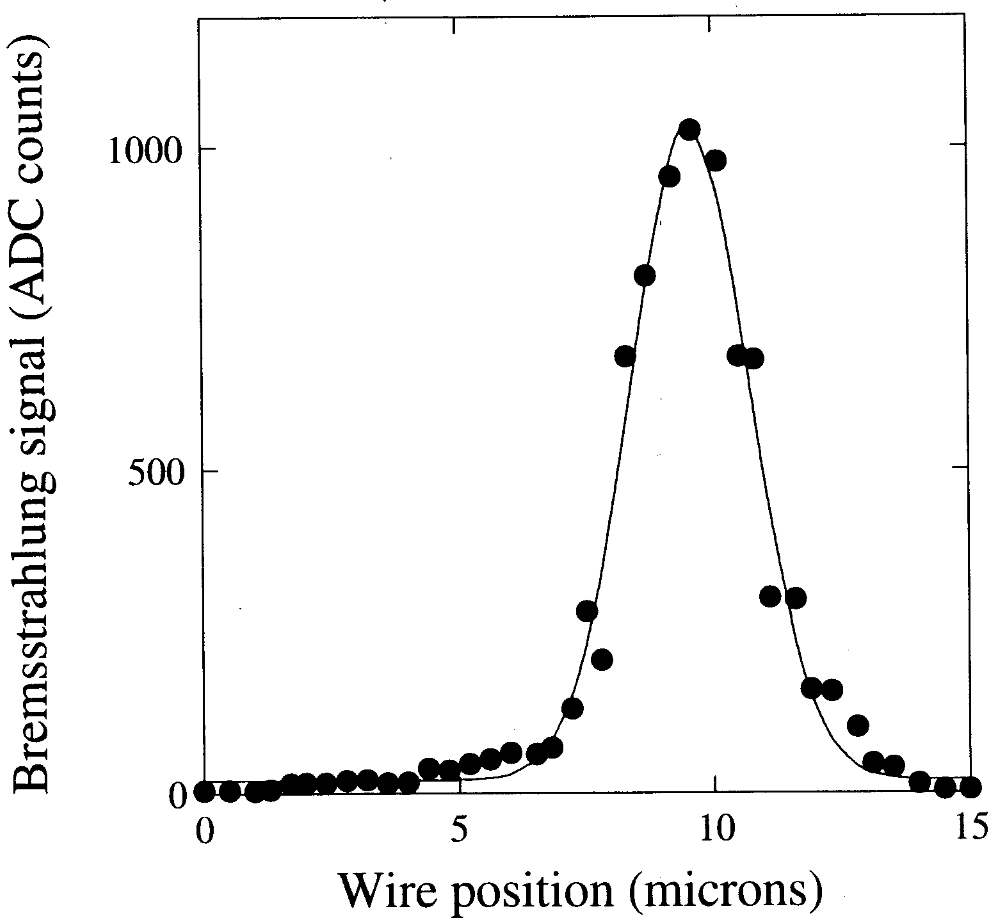
Bremsstrahlung signal (ADC counts)
1000
500
0
0
5
10
15
Wire position (microns)

Fig. 6

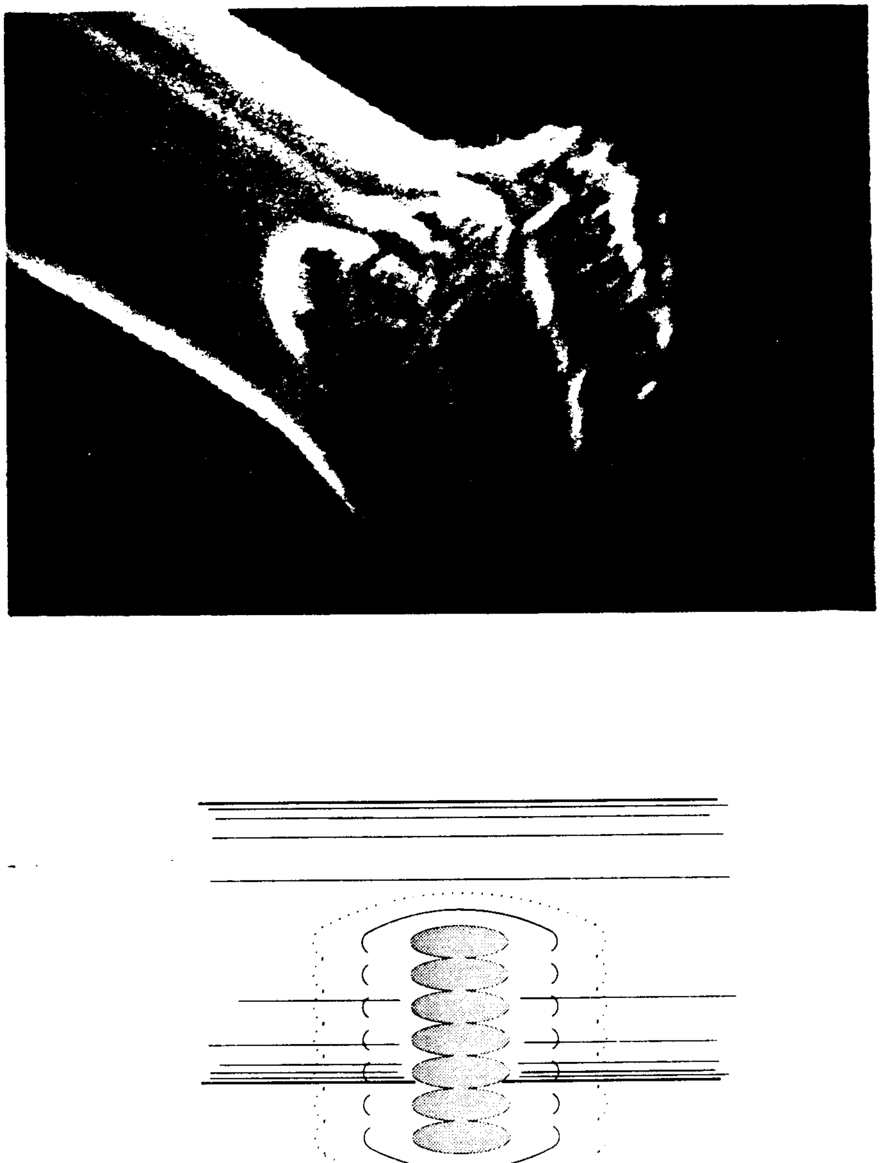

11-94 7841A14

Fig. 7

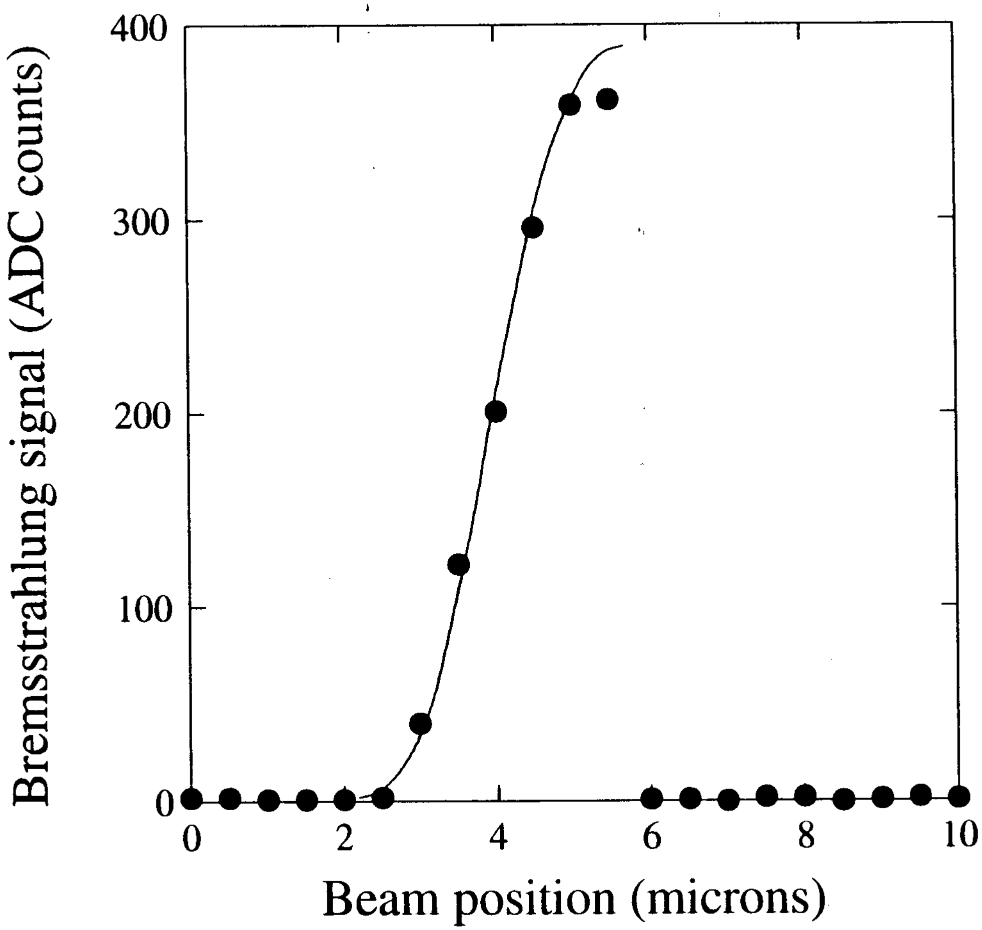
Bremsstrahlung signal (ADC counts)
400
300
200
100
0
0
2
4
6
8
10
Beam position (microns)

Fig. 8

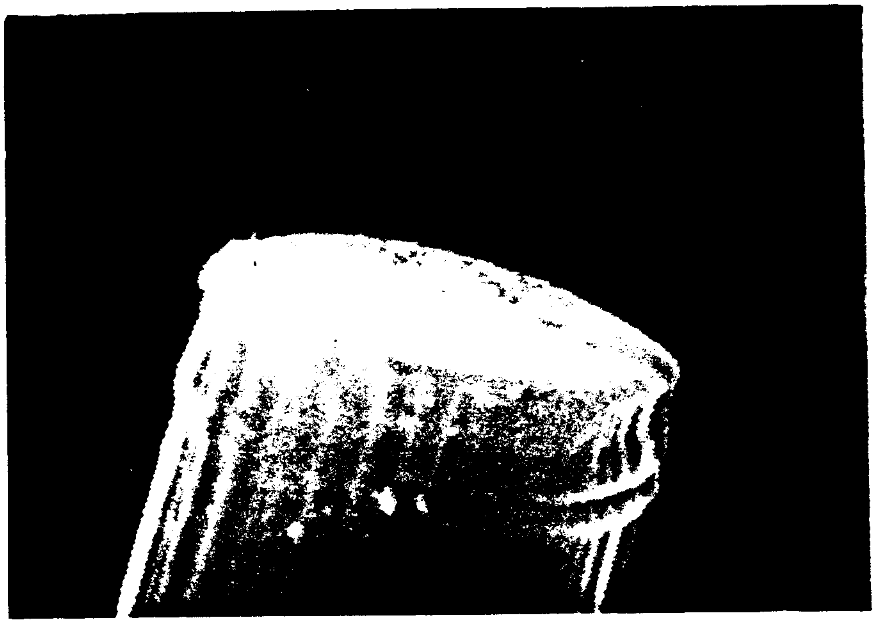

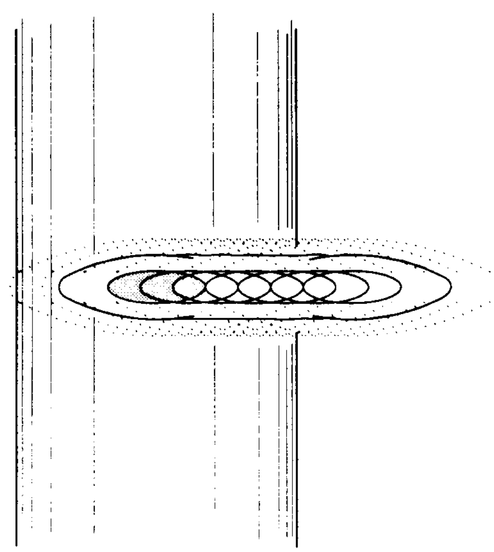

11-94 7841A13

Fig. 9

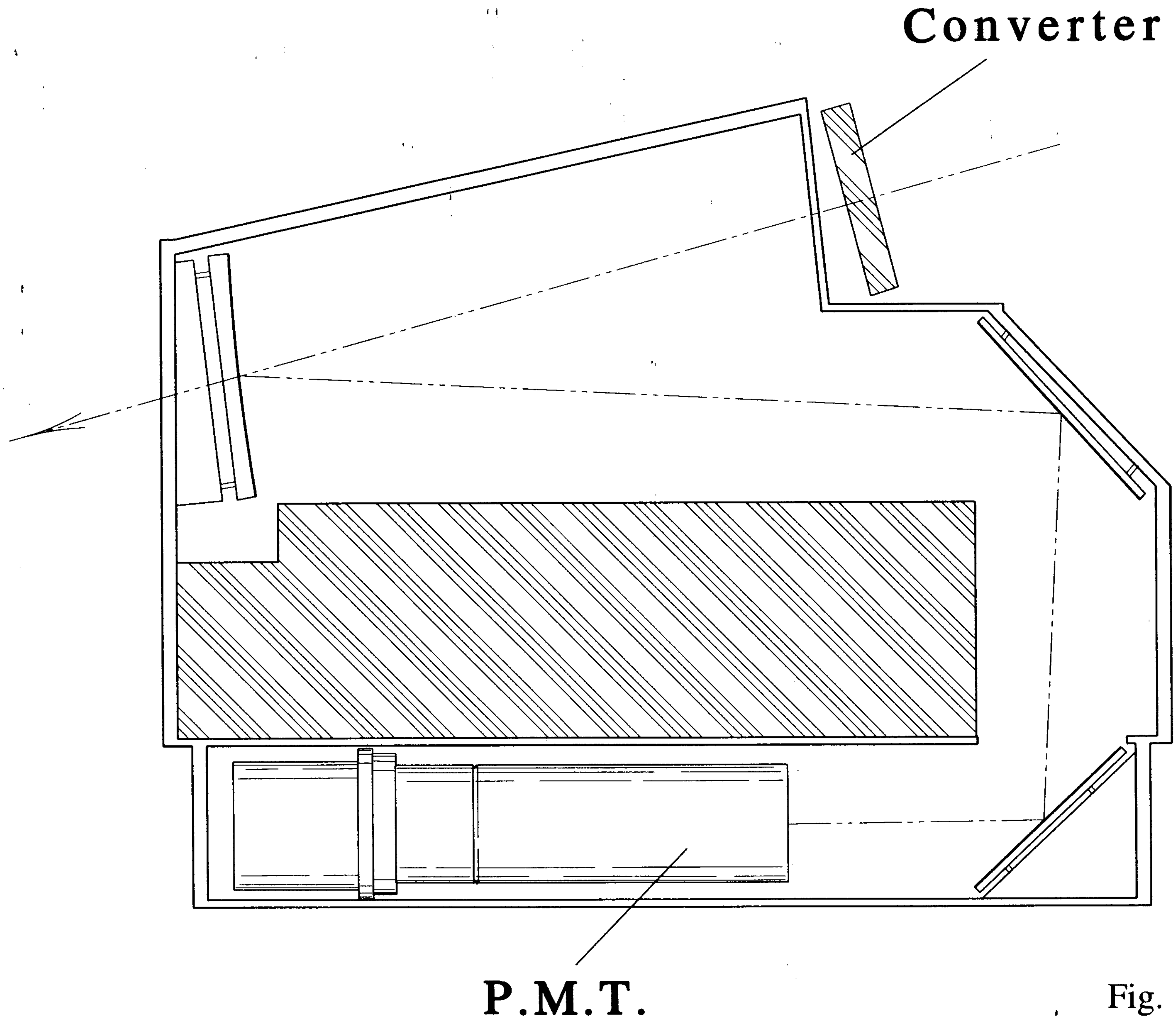

Fig. 10

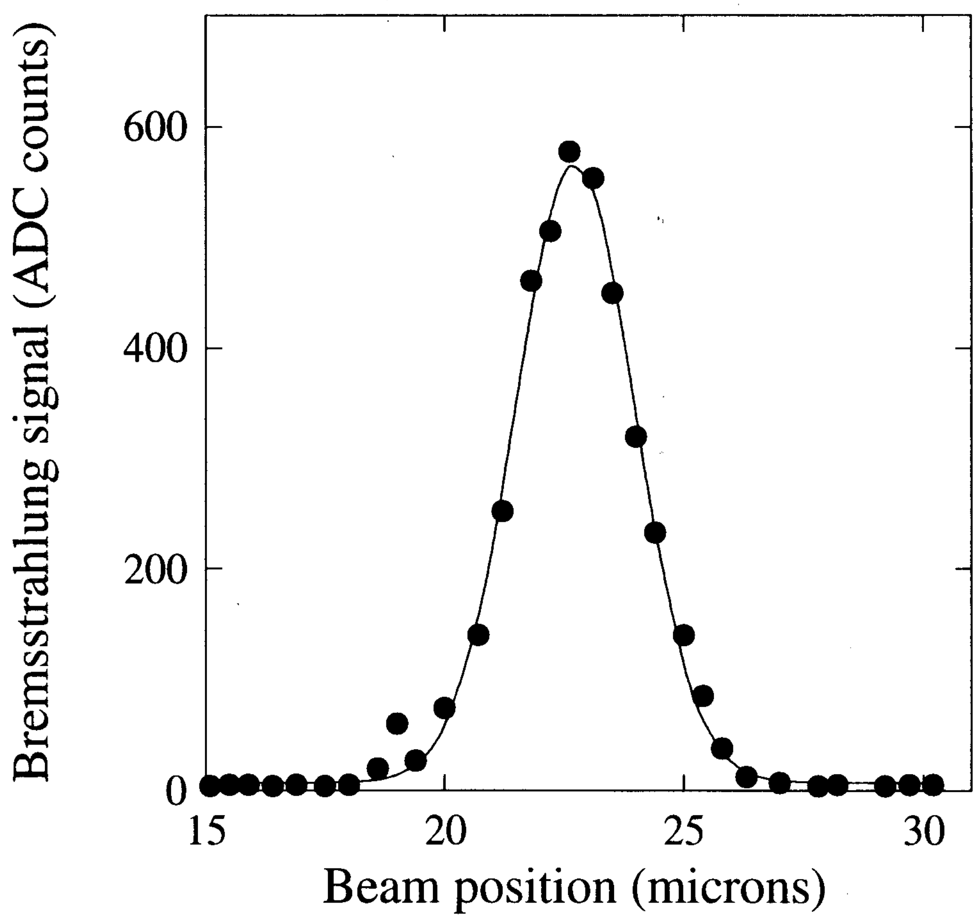
Bremsstrahlung signal (ADC counts)
600
400
200
0
15
20
25
30
Beam position (microns)

Fig. 11

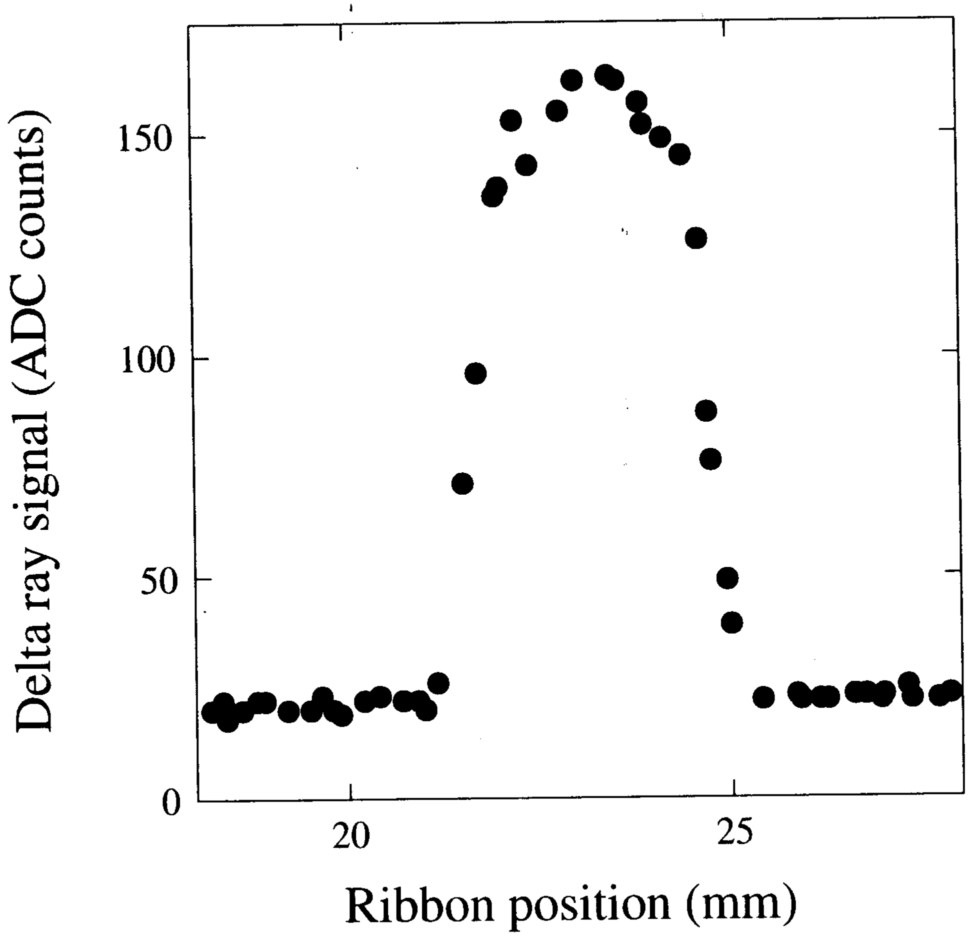

Delta ray signal (ADC counts)
0
50
100
150
20
25
Ribbon position (mm)

Fig. 12

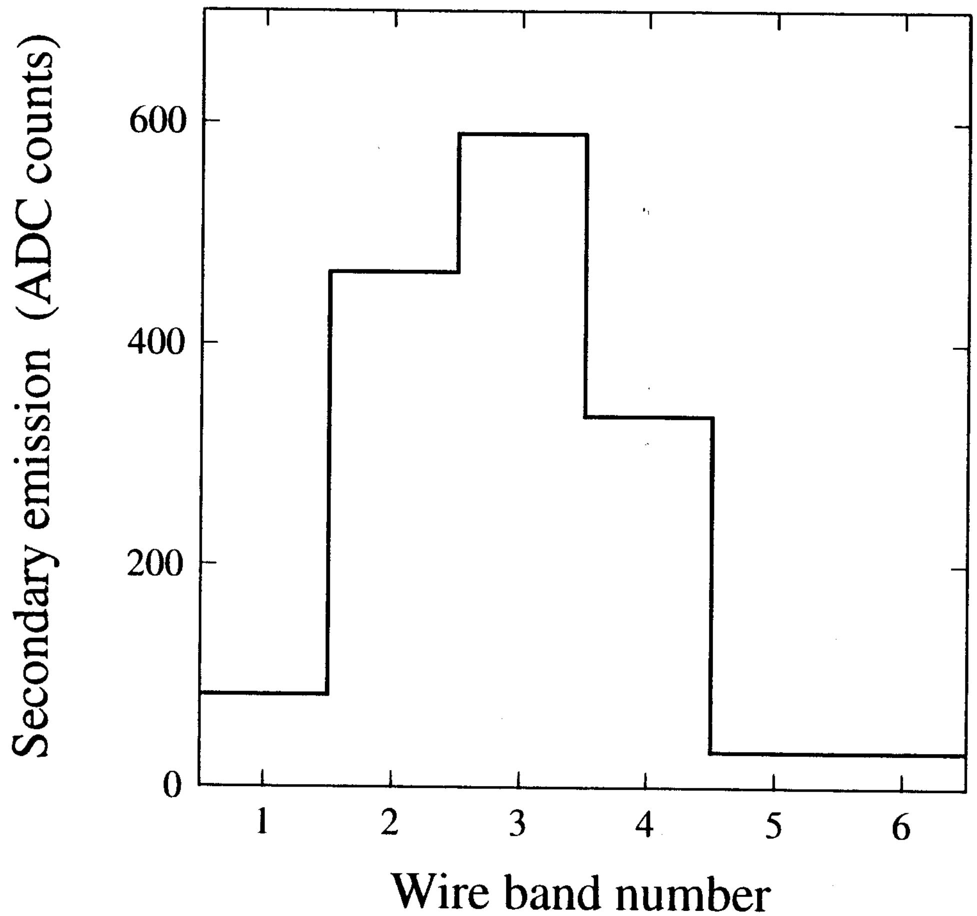
Secondary emission (ADC counts)
600
400
200
0
1
2
3
4
5
6
Wire band number

Fig. 13